Structural and properties of Zn-Al_2O_3-SiC nano-composite coatings by direct electrolytic process

O. S. I. Fayomi, A. P. I. Popoola & O. E. Olorunniwo

The International Journal of Advanced Manufacturing Technology

ISSN 0268-3768

Int J Adv Manuf Technol
DOI 10.1007/s00170-016-8428-4

Springer

Int J Adv Manuf Technol
DOI 10.1007/s00170-016-8428-4

ORIGINAL ARTICLE

Structural and properties of Zn-Al_2O_3-SiC nano-composite coatings by direct electrolytic process

O. S. I. Fayomi[1,2] · **A. P. I. Popoola**[1] · **O. E. Olorunniwo**[1,3]

Received: 9 September 2015 / Accepted: 25 January 2016

Abstract In this paper, Zn-SiC and Zn-Al_2O_3-SiC composite coating were fabricated by electrodeposition technique from sulfates bath. The resulting composite coating was carried out by adding Al_2O_3/SiC particulate to a zinc-containing bath. The properties of the composite coating were investigated by SEM equipped with EDS, XRD, and AFM. The electrochemical behavior of the coating alloy was evaluated in 3.65 % NaCl with linear polarization technique and mechanically examined by durascan microhardness tester. The morphology of the thermal treated coatings at 400 °C in 6 h was viewed with high optical microscope (OPM). The results show hardness, thermal stability, and anti-corrosion properties of Zn-Al_2O_3-SiC were improved significantly as against Zn-SiC coating matrixes. This was attributed to dispersive strengthening effect and grain induced effort of Al_2O_3/SiC particulate. The decrease in corrosion and thermal stability at 15 g/L of SiC concentration may be as a result of agglomeration and the superimposed particle in the plating bath.

Keywords Microstructure · Zn-Al_2O_3-SiC · Micro-hardness · Interfacial effect · Thermal stability

✉ O. S. I. Fayomi
ojosundayfayomi3@gmail.com

[1] Department of Chemical, Metallurgical and Materials Engineering, Tshwane University of Technology, P.M.B. X680, Pretoria, South Africa

[2] Department of Mechanical Engineering, Covenant University, P.M.B. 1023, Ota, Ogun State, Nigeria

[3] Department of Materials Science and Engineering, Obafemi Awolowo University, Ile-Ife, Nigeria

1 Introduction

The existence of Zn coating over the years has tremendously been attested to exhibit resilient mechanical and corrosion resistance to a considerable level [1–4]. Meanwhile, their service performance decreases due to scar piled up in mechanical application and aggressive medium resulting from corrosion product [4–7]. Metal and ceramics composite deposition are appreciated surface modification technologies to obtain significant reinforced properties. Their engineering relevance varied based on the individual characteristics such as wear resistance, increase in stiffness, high temperature properties, good strength behavior, and enhanced corrosion properties. The majority of this characteristic plays a priority in machinery, chemical industry, light space application, automobile, defense, spaceflight aviation, and photonics [8–12].

An effort to enhance the promising option for zinc-based alloy instead of passivation technique is the introduction of dispersed composite and nano-composite materials like TiO_2, SiO_2, ZrO_2, CNTs, WC, Al_2O_3, and SiC which are extensively used to modify coating and electrode. Some report by authors attested that composite coating with silica and mica particle in Zn interface increased hardness and considerable improvement in corrosion resistance properties [11–15]. Incorporation resulted in higher anti-corrosion properties that were also achieved with Al_2O_3 in Zn-Ni intermediate [16].

This composite induced metal and ceramic particle possess outstanding performance with composition in both metal and the second phase particulate. Considerable study has been carried out in view to develop suitable materials for severe service life performance where excellent tribological properties, weight reduction,

Published online: 22 February 2016

better compatibility, and good hardness behavior could be accessed. One of the substantial factors for improved hardness and recrystallization behavior is thermal stability. Thermal treatments are known to alter the physical and chemical behavior of materials. They provide significant case hardening and give manipulating properties such as hardness, strength, toughness, ductility, and elasticity. In view of this, silicon carbide is considered as a major particulate. SiC is an excellent abrasive composed of tetrahedral of carbon and silicon atoms with strong bonds in the crystal lattice [17–19]. This produces a very hard and strong material. Silicon carbide is not attacked by any acids or alkalis or molten salts up to 800 °C. The high thermal conductivity coupled with low thermal expansion and high strength gives this material exceptional thermal shock resistance qualities [20–24].

The nucleation growth and mechanical and adhesion properties of Zn-Al_2O_3-SiC have not been studied in detail in sulfate environments to the best of our knowledge. The objective of the work is to develop a particulate-strengthened bright and adherent Zn-Al_2O_3/SiC deposit, and observe the morphological features, mechanical and thermo-mechanical properties, corrosion, and adhesion efficiency performance of the developed coatings. This attention in ceramic composite is significant because of the roles in engineering and various applications in recent time.

2 Experimental procedure

2.1 Preparation of substrate

Mild steel specimens of sheet dimension 30 × 20 × 1 mm were used as substrate and zinc sheets of 40 × 30 × 2 mm were prepared as anodes. The initial surface preparation was performed with finer grade of emery paper as described in our previous studies [8, 12]. The sample were properly cleaned with sodium carbonate, pickled, and activated with 5 % HCl at ambient temperature for 10 s followed by instant rinsing in deionized water. The mild steel specimens were obtained from a metal sample site in Nigeria. The chemical composition of the sectioned samples is shown in Table 1 as obtained from spectrometer analyzer.

2.2 Formation of deposited coating

The mild steel substrate earlier prepared was actuated by dipping into 10 % HCl solution for 10 s followed by rinsing in distilled water. Analytical grade chemicals and distilled water were used to prepare the plating solution at room temperature prior to plating. The formulations were then placed in a stirrer for a day while heated to 40 °C to easily admix and to allow for dissolution of any agglomerate in the bath solution. The bath produced from the formulation in Table 2 is concurrently stirred as heating trend lasted for hours before plating [8].

Table 1 Nominal chemical composition (wt.%) of mild steel substrate

Element	C	Mn	Si	P	S	Al	Ni	Fe
% Composition	0.15	0.45	0.18	0.01	0.031	0.005	0.008	Balance

2.3 Preparation of the coatings

The prepared Zn-Al_2O_3-SiC bath composite was heated for 2 h and intermittently stirred to obtain clear solution before it was prepared by electrolytic deposition process over mild steel. The prepared cathode and anodes were connected to the DC power supply through a rectifier as presented in Fig. 1. Deposition was carried out at varying applied currents between 0.5 and 1.0 A for 15 min.

The distance between the anode and the cathode and the immersion depth was kept constant. Thereafter, the samples were rinsed in water and dried. The formulated design plan for the coating is described in Table 3.

2.4 Structural characterization of the coatings

The structural studies and elemental analysis of the fabricated alloy samples were verified using a TESCAN scanning electron microscope with an attached energy dispersive spectrometer (SEM/EDS) and an optical microscope (OM). The phase property was observed with the help of x-ray diffractogram. The adhesion profile, topography, and morphology of the coating were observed with the help of atomic force microscope (AFM). High optic diamond-based durascan micro-

Table 2 Bath composition of Zn-Al_2O_3-SiC alloy co-deposition matrix

Composition	Mass concentration (g/L)
$ZnSO_4 \cdot 7H_2O$	70
Al_2O_3	5–10
SiC	10–15
Boric acid	5
Glycine	5
Thiourea	5
Temp	40 °C
pH	3.5–4.2
Time	15 min
Current	0.5–1.0 A

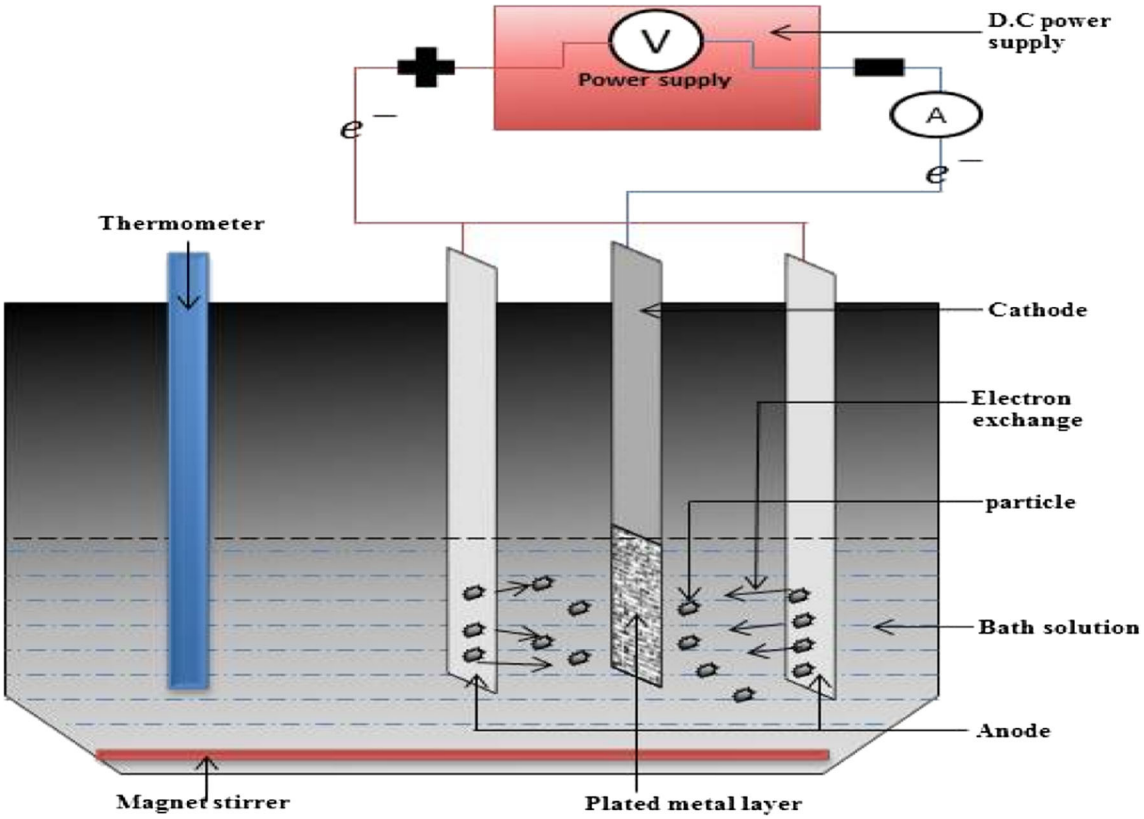

Fig. 1 Schematic diagram of electrodeposited system

hardness tester was used to estimate the average microhardness of the deposit in an equal interval range.

2.5 Thermo-/electro-oxidation test

Isothermal heat treatment (direct fired furnace atmosphere) of Zn-Al_2O_3-SiC composite coating was carried out at 400 °C for 6 h to check the mechanical stability of the coated samples. The electrochemical studies were performed with Autolab PGSTAT 101 Metrohm potentiostat using a three-electrode cell assembly in a 3.65 % NaCl static solution at 40 °C. The developed composite was the working electrode, platinum electrode was used as counter electrode, and Ag/AgCl was used as reference electrode. The anodic and cathodic polarization curves were recorded by a constant scan rate of 0.012 V/s which was fixed from ±1.5 mV. From the Tafel corrosion analysis, the corrosion rate and potential and linear polarization resistance were obtained.

Table 3 Formulated designed bath composition of Zn-Al_2O_3-SIC

Sample order	Matrix sample	Current density (A/cm^2)
1	Zn-5Al_2O_3-10SiC	0.5
2	Zn-5Al_2O_3-10SiC	1.0
3	Zn-10SiC	0.5
4	Zn-10SiC	1.0
5	Zn-15SiC	0.5
6	Zn-15SiC	1.0
7	Zn-10Al_2O_3-15SiC	0.5
8	Zn-10Al_2O_3-15SiC	1.0

3 Results and discussion

3.1 SEM/EDS of deposited alloy

Figures 2 and 3 show the SEM/EDS structure of represented Zn-Al_2O_3-SiC fabricated ceramic coating with reference to Zn-15SiC and Zn-10Al-15SiC matrix, respectively. From the two figures, it is obvious that the crystal flakes of the deposits were homogeneously dispersed on the interface. It is quite evident that at 1.0 A for Zn-15SiC, a noticeable crystal nucleus patched along the interface was observed. Apparently, there are two distinctive phases, the initial having a homogeneously uniform stable precipitate and the latter with hexagonal patches. In fact, the incorporation of the SiC along the zinc

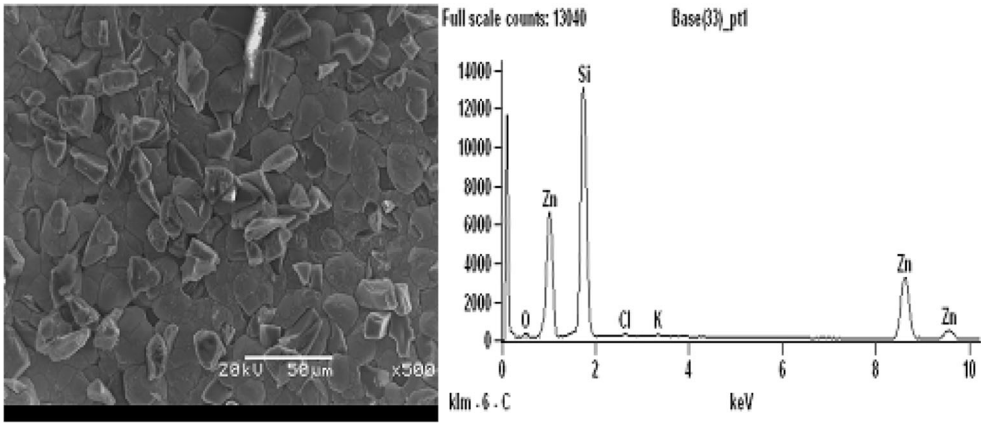

Fig. 2 SEM/EDS micrographs of Zn-15SiC sample

interfacial could be seen to provide a refine microstructure with dominating nodular particle.

The deposition appearance with coating interferes of Al_2O_3/SiC was quite appreciated in that both particulate strengthened composites find their way expressly doped into the zinc metal matrix. The structural behavior was quite expected because the nucleation process proceeds from the zinc metal as load bearer and the dispersion of the particulate covers the nucleation site and strengthens the produced alloy [17] (Fig. 3).

In other words, it is necessary to mention that morphological change may be associated to the strong blocking influence of the induced composite leading to good precipitation and better orientation. Sometimes, the conditioning parameter in relation to the degree of additive impediment also plays a vital role in the re-modification of the crystal orientation and surface texture of the deposit as attested by [3].

Figure 4 shows the XRD pattern of the Zn-Al_2O_3-SiC deposit prepared with 10Al_2O_3/15SiC nanoparticle concentration from the plating bath. The diffractogram gives the major diffraction peak as 38, 42, 45, 55, and 72°. The intermetallic growth phases observed are Zn, Zn_2Al_7 Zn_2Si etc. The presence of the individual dispatched metal-particulate phases was noticeable on the coating as it seems to influence the phase change through the help of inter-diffusion mechanism and ion of each particulate [24]. The phase orientations of the metal matrix are an indication of the harness performance and remarkable effect of the coating produced.

3.2 Atomic force microscope analysis

Figures 5, 6, 7, and 8 show the atomic force micrographs of the composite coating with their surface roughness and topography. With Figs. 5 and 7, two distinct phases were observed along the interface. The gray area indicates the interference of the SiC embedded within the zinc matrix. The other phase is the zinc major. The particle seems to be dubbed within the inter-link inform of grain. However, the dispersion was regular and the topography is quite appreciable. For the ternary alloy series, Zn-Al_2O_3-15SiC in Figs. 6 and 8, the deposit shows a well-dispersed and homogeneous topography uniformly distributed with undulation like the binary composite coating.

The better topographical modifications of the crystal growth are attributed to the perfect precipitation and well-defined intermediate phases obtained. Another

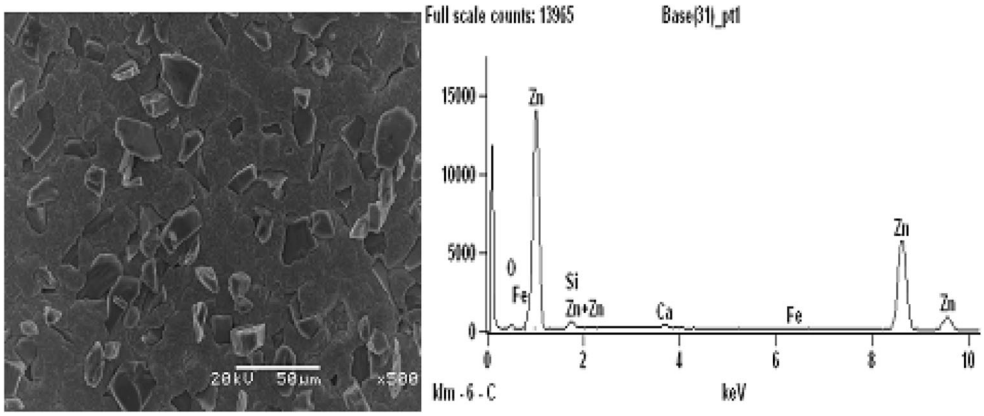

Fig. 3 SEM/EDS micrographs of Zn-10Al_2O_3-15SiC sample

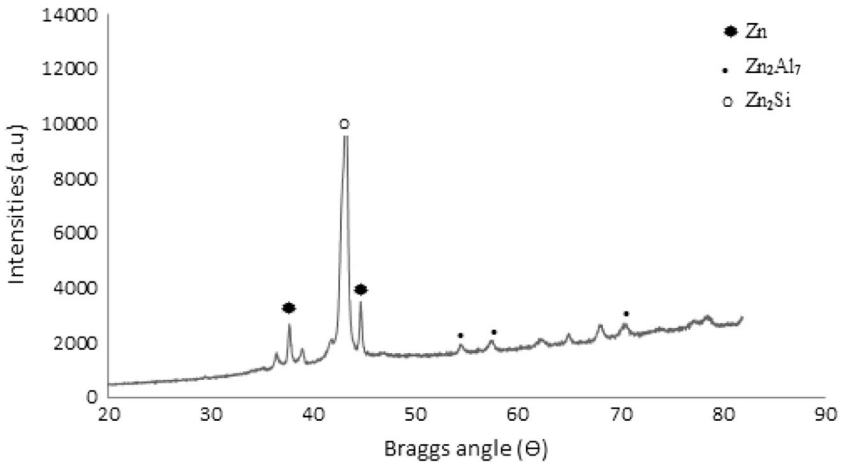

Fig. 4 XRD pattern of Zn-$10Al_2O_3$-15SiC sample

important point to note is that diffusion of ions of individual composite particulate into the nucleus and lattices of the cathode are not only influenced by the composite characteristics but also the process parameter [8, 11]. In view of this, the better zinc distribution along with Al_2O_3-15SiC provides a robust distribution expected and less agglomeration of particulate was seen.

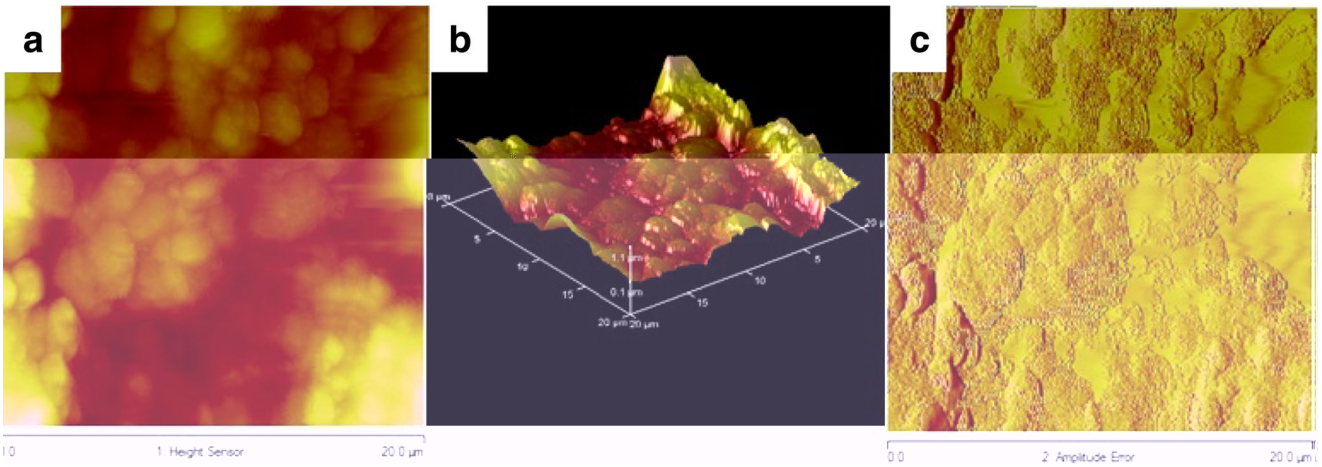

Fig. 5 AFM images of Zn-15SiC deposited on mild steel

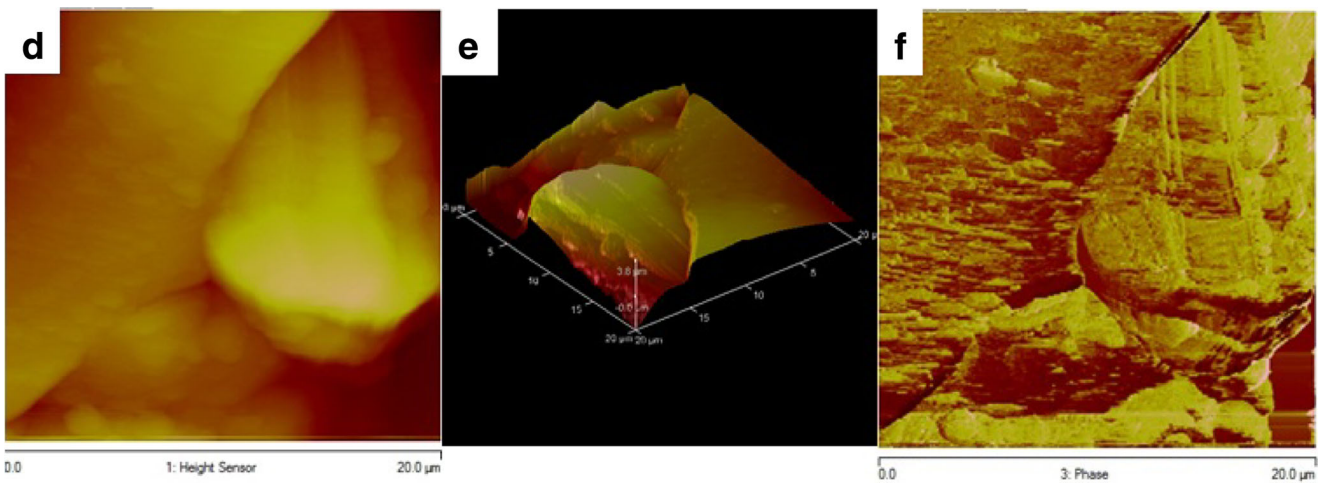

Fig. 6 AFM images of Zn-Al_2O_3-15SiC deposited on mild steel

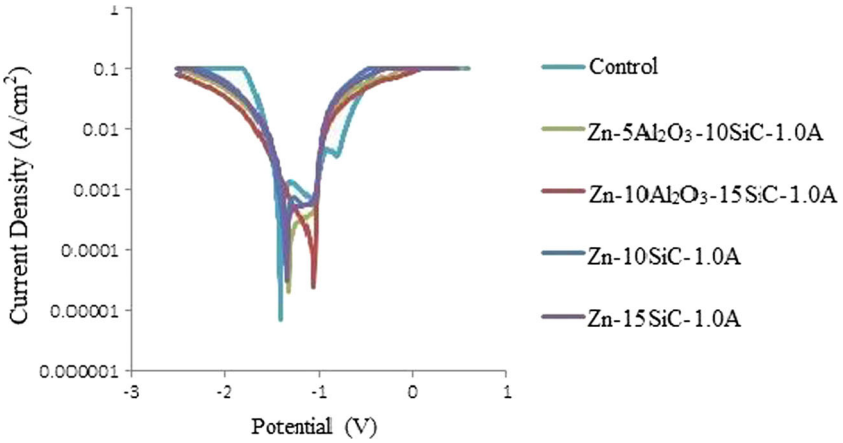

Fig. 7 Linear potentiodynamic polarization curve of coatings at 1.0 A

3.3 Potentiodynamic polarization studies

Polarization test was studied in 3.65 % NaCl solution. The Tafel plots acquired for the coating are shown in both Figs. 9 and 10 with their respective polarization value. The anodic and cathodic site Tafel value and corrosion current density derived after extrapolations are given in detail in Tables 4 and 5. The corrosion current (I_{corr}), corrosion potential (E_{corr}), and corrosion rates (CR) were obtained from the Tafel plots and are recorded. The corrosion rates (CR) were calculated by the following equation.

$$\mathrm{CR(mpy)} = 0.13\mathrm{Icorr\ (Eq.wt.)/D}$$

As can be seen, composite coating has a less negative corrosion potential value and smaller corrosion current densities than the control mild steel sample. To match the composite deposited fabricated coatings, the corrosion potential values of the composite layers from the solution containing Zn-10Al_2O_3-15SiC (1.0A) gave a less negative value than the Zn-SiC alloys, indicating that the Zn-SiC coating extensively interacts with the cathodic activities. This significant positive change in potential of the Zn-10Al_2O_3-15SiC (1.0A) as obtained in Figs. 5 and 7 and Table 4 is attributed to the modifications induced on the deposit's surface by the particle co-deposition. This puts forward the presence of Al_2O_3/SiC particle in zinc coating, which influences the kinetics of electrochemical processes.

On the other hand, it is important to mention that decreases in corrosion current density were observed for the Zn-10Al_2O_3-15SiC deposited at 1.0 A as compared to 0.5A, meaning that deposition power and the concentration of additive in the metal deposits determine the inhibitive influence and the metal degradation phenomena of any deposited coatings which is in agreement with results obtained by [11, 25]. In literature, the positive shift of E_{corr} indicates an increase or a better resistance of a material, thus in Figs. 6 and 8 and Table 5, the matrix of Zn-15SiC deposited in 0.5 V shows an improvement in E_{corr} when compared to the as-received sample, but low resistance when compared to other co-deposited samples. The Zn-10Al_2O_3-15SiC sample indicated better corrosion potential of −1.3047 V.

The coatings, however, improved the corrosion resistance of the mild steel substrate, with significant polarization

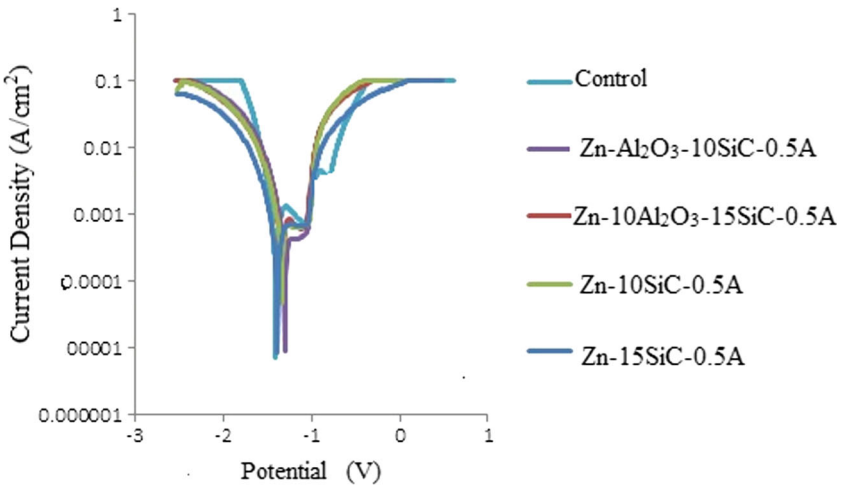

Fig. 8 Linear potentiodynamic polarization curve of coatings at (0.5 V)

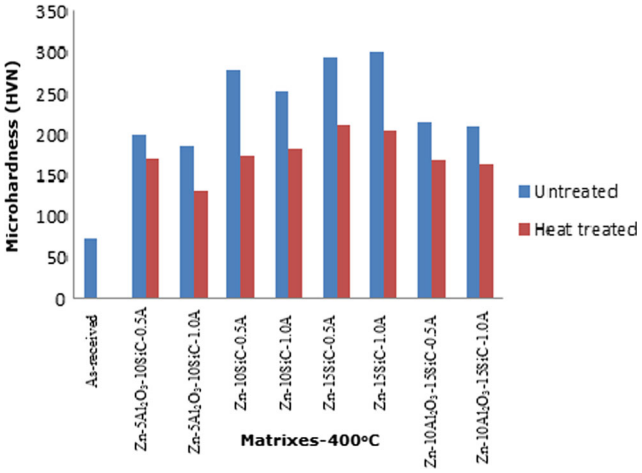

Fig. 9 Microhardness trend of untreated and heat treated coating at 400 °C for 6 h

resistance of 205.51 Ω. This indicates that the admixed coating matrixes are promising for enhancing the substrate material, but must be restrained to certain potential of coating to enforce compactness and cohesion. More so, it is important to note the activities on alumina as these relate to the interference of the zinc metal particles of all coatings of concern. The anti-corrosion properties were observed to be fascinating in all alumina induced, and the reason might be because alumina particles have a low level of electronic conductivity and when dispersed in bath they provide essential distraction for corrosion quickening to occur [25, 26].

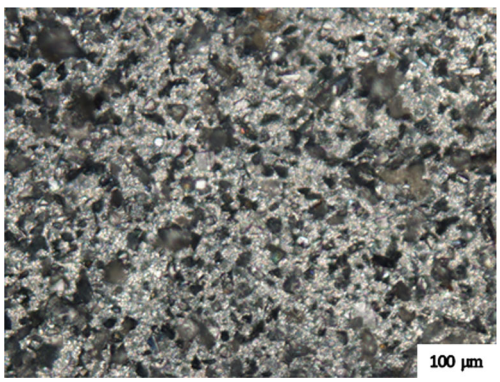

Fig. 10 Microstructure of Zn-10Al_2O_3-15SiC sample after heat treatment at 400 °C for 6 h. The structure reveals the precipitation and uniform distribution of $ZnSiAl_5$ phase

3.4 Microhardness analysis/thermo-mechanical studies

The effect of heat treatment on the microhardness properties of deposited ceramics composite coating under varied deposited condition in order to verify its mechanical stability is presented in Fig. 9. In general, all as-deposited coatings still perform invariably well as against the as-received MS sample with 65HVN. Two critical performance behaviors were observed among the fabricated deposits before heat treatment; firstly, SiC particulate in its single incorporation into the zinc matrix (Zn-SiCs) seems to perfectly produce a harder surface thereby altering barrier to plastic deformation and enhancing hardness characteristic. In the second observation for the Zn-SiC in the presence of Al_2O_3, significant hardness properties were also attained for all variations which is in accordance to the report by [27] and our previous studies [12, 25] on the effort of alumina in strengthening zinc metal.

However, the hardness properties of Zn-Al_2O_3-SiC coating (205HVN) are lesser than the silica conditioned matrix (305HVN); this might be as a result of particle loadings and agglomeration which loosely adheres with the matrix and thereafter fell off the deposit, leading to appearance of unwanted gaps and pores [15]. Interestingly, when such occurrences occur, distortion is certain. Though from some literature heat treatment helps to increase microhardness, it is also evident from our studies that it depends on the deformation time. After heat treatment at 400 °C in 6 h, the degree of response to deformation and transformation in hardness behavior reduces for Zn-SiC alloy series with pile up as compared to Zn-Al_2O_3-SiC with little change in microhardness. The ratio of diminishing at 6 h of heat treatment for Zn-SiC and Zn-Al_2O_3-SiC matrixes is 80:30 at 220HVN:175HVN, respectively. The effect of Al_2O_3/SiC refinement and perfect precipitate has been perhaps seen to justify a substantial stability of the coating even at less hardness as compared to Zn-SiC matrix coatings.

The microstructure of the as-deposited Zn-10Al_2O_3-15SiC and Zn-15SiC representing the matrixes is thermally heat treated at 400 °C for 6 h and is presented in Figs. 10 and 11 by the use of metallurgical optical microscope. The

Table 4 Tafel polarization data of Zn-SiC and Zn-Al_2O_3-SiC alloy at 1.0 A co-deposition matrix

Matrix	E_{corr}, obs (V)	j_{corr} (A/cm^2)	C_R (mm/year)	R_P (Ω)
Zn-5Al_2O_3-10SiC (1.0 A)	−1.3081	6.63E−05	0.7702	196.36
Zn-10Al_2O_3-15SiC (1.0 A)	−1.0544	4.51E−05	0.52422	229.22
Zn-10SiC (1.0 A)	−1.3505	0.000107	1.2462	117.05
Zn-15SiC (1.0 A)	−1.3322	0.000102	1.1813	114.24
Control	−1.53900	7.04E−02	4.1000	27.600

Table 5 Tafel polarization data of Zn-SiC and Zn-Al_2O_3-SiC alloy at 0.5 A co-deposition matrix

Matrix	E_{corr}, obs (V)	j_{corr} (A/cm^2)	C_R (mm/year)	R_P (Ω)
Zn-5Al_2O_3-10SiC 0.5 A	−1.3047	6.36E−05	0.73898	205.51
Zn-10Al_2O_3-15SiC 0.5 A	−1.3392	8.48E−05	0.98575	109.78
Zn-10SiC-0.5 A	−1.3448	0.000101	1.1743	99.383
Zn-15SiC-0.5 A	−1.3919	0.000105	1.2217	85.036
Control	−1.53900	7.04E−02	4.1000	27.600

microstructure of the Zn-10Al_2O_3-15SiC heat treated samples reveals satisfactorily a uniform distribution and enhanced precipitation of SiC and Al phase as observed in Fig. 10.

More so, the intermetallic phase such as $ZnSiAl_5$ is apparent due to the secondary dispersed composite particle. The microstructure for Zn-SiC matrix in Fig. 11 was not well distributed as compared to the formal, although a continuous silica interference was seen within the coating interface in little patches. As previously mentioned, the effect of particle loading and good admixed additive blend into the interfacial lattice of the zinc metal could be the basis for the sustained and good crystal transformation of the Zn-10Al_2O_3-15SiC coating after such heat treatment process.

4 Coating adsorption mechanism and coating efficiency

Particle entrapments into the metal lattices take place through the mechanism of adsorption which entails but is not limited to particulate dissolving capacity, the formation of solid precipitation at interface, the particle surface area, good throwing power, and Interpol of the individual elemental feature. Hence, these characteristics should give better coating efficiency. However, from our studies, we foresee that the dissolving capacity is a function of mass of dissolving particle on the base solution and inversely proportional to the surface area, throwing power, and time of deposition. Therefore, the assumed prediction equation might be

$$V\&M\& \frac{1}{AWT} \tag{1}$$

where V is the dissolving capacity, M is the mass of the dissolving particulate, A is the surface area, and W is the throwing potential or current density. Hence,

$$V\&M\& \frac{1}{AWT} \tag{2}$$

More so, since the efficiency of a coating is not determined alone by physical properties but also to the resilient chemical and mechanical resistance behavior of the deposit, a purposeful relationship with corrosion propagation and possible progression was proposed to justify the coating efficiency. Therefore, for CE% PP_{icorr} and CE% PP_{Rp}, the below relationships are illustrated in Eqs. 3 and 4, respectively.

$$\text{CE}\ (\%) = \text{PP}_{\text{icorr}} = \frac{icorr(control) - icorr(A)}{icorr(control)} \times 100 \tag{3}$$

$$\text{CE}\ (\%) = \text{PP}_{\text{RP}} = \frac{RP(A)RP(control)}{RP(A)} \times 100 \tag{4}$$

Figures 12 and 13 present a chart of coating efficiency (CE %) obtained from deposited matrix in accordance with stipulated developed equations. The parameters like potentiodynamic polarization-corrosion density (PP-Icorr) and potentiodynamic polarization resistance (LPR) from corrosion Tafel extrapolation (see Tables 4 and 5) were used to compute the chart in Figs. 12 and 13.

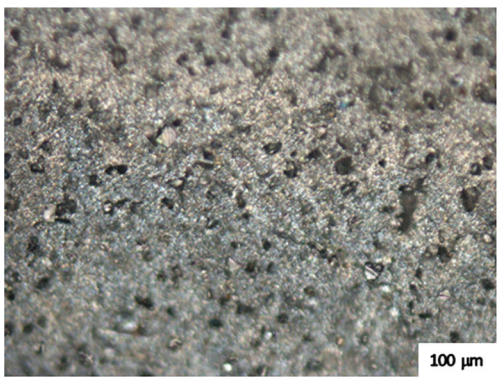

Fig. 11 Micrographs of Zn-15SiC sample after heat treatment400°C for 6 h. The structure reveals the precipitation and uniform distribution of Zn_2Si phase

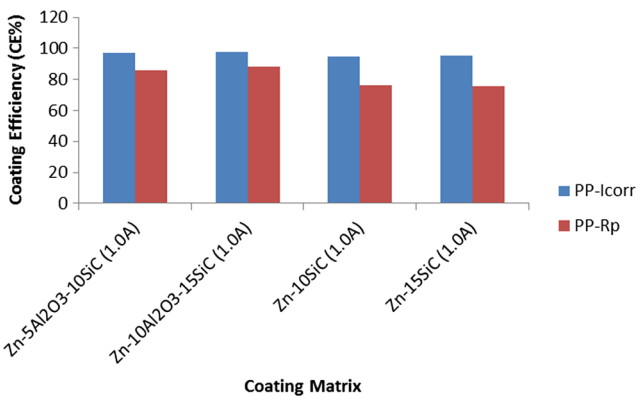

Fig. 12 Coating efficiency (CE %) of obtained deposited matrix at 1.0 A in relation to PP-Icorr and PP-LPR

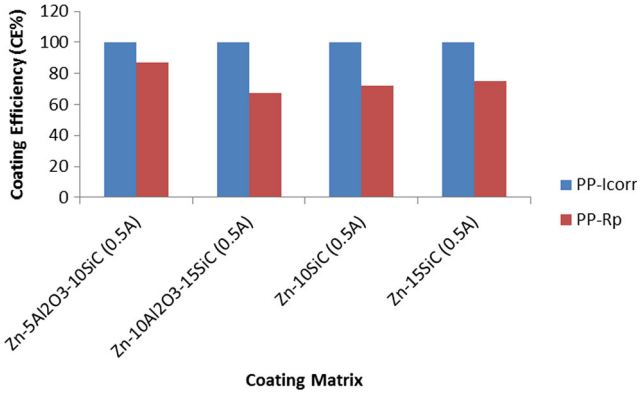

Fig. 13 Coating efficiency (CE %) of obtained deposited matrix at 0.5 A in relation to PP-Icorr and PP-LPR

From the comparative examination, it was apparent that the coating efficiency from all processes agreed and showed improved properties especially with the ternary alloy composite coating as against binary phase. With PP-Rp 97.8 %, PP-Icorr 87.9 % for Zn-10Al_2O_3-15SiC alloy at 1.0 A, the binary matrix Zn-15SiC possesses PP-Rp 95 %, PP-Icorr 75 % coating efficiency. The adsorption characteristics and incorporation of the metal lattices can be seen to center around the interfacial and the atom of admixed particulate [9, 10].

5 Conclusions

1. Al_2O_3/SiC have been successfully co-deposited with Zn metal matrix to fabricate Zn-Al_2O_3-SiC composite coating.
2. Uniform distribution of the Al_2O_3/SiC in the microstructure of both Zn-SiC and Zn-Al_2O_3/SiC coating is an essential factor responsible for the improvement in structural and mechanical properties.
3. Heat treatment of Zn-Al_2O_3/SiC composite coating results in crystallite formation. The hardness and the coating efficiency greatly increase as a result of the embedded Al_2O_3/SiC which produced a $ZnSiAl_5$ and Zn_2Si phase in the composite coating at 400 °C
4. The anti-corrosion resistance property of the coating increased significantly. The corrosion resistance increases with the increase in additive concentration.

Acknowledgments This material is based upon work supported financially by the National Research Foundation. The authors acknowledge the support from Surface Engineering Research Centre (SERC), Tshwane University of Technology Pretoria South Africa.

References

1. Amuda A et al (2009) Study of optimum conditions of zinc plating on mild steel. Inter J Eng Res Afr 2:31–39
2. Elsherief AE, Shoeib MA (2003) Characterization of electrodeposited Zn-Ni alloy from an all-chloride solution. Corr Preven Control 50:25–30
3. Fayomi OSI, Popoola API (2013) Interfacial effect and the microstructural characterization of the induced zinc–aluminum–*Solanum tuberosum* in chloride solution on mild steel. Res Chem Inter 39: 1354–1362
4. Fayomi OSI et al (2012) Morphology and properties of Zn-Al-TiO_2 composite on mild steel. Proc. ICCEM 207–210
5. Basavanna S, Arthoba NY (2009) Electrochemical studies of Zn–Ni alloy coatings from acid chloride bath. J Applied Electro 39(10): 1975–1982
6. Chitharanjan HA, Venkatakrishna K, Eliaz N (2010) Electrodeposition of Zn–Ni, Zn–Fe and Zn–Ni–Fe alloys. Surf Coat Tech 205:2031–2041
7. Dikici T, Culha O, Toparli M (2010) Study of the mechanical and structural properties of Zn–Ni–Co ternary alloy electroplating. J Coat Tech Res 7(6):787–792
8. Fayomi OSI, Popoola API (2012) An investigation of corrosion and mechanical behaviour of Zn coated mild steel in 3.65% NaCl. Inter J Electrochem Sci 7:6555–6570
9. Mohankumar C et al (2012) Electro-deposition and corrosion behavior of Zn–Ni and Zn–Ni–Fe_2O_3 coatings. J Coat Technol Res 9(1):71–77
10. Mou H et al (2010) Effect of LC-refining on fiber surface chemistry of eucalyptus. Nov 8th, 4th ISETPP, Guangzhou
11. Fayomi OSI, Popoola API, Popoola OM (2012) Comparative studies of microstructural, tribological and corrosion properties of plated Zn and Zn-alloy coatings. Inter J Electrochem Sci 7:4860–4870
12. Fayomi OSI, Popoola API, Popoola OM (2012) Electrochemical and mechanical properties of mild steel electroplated with Zn-Al. Inter J Electrochem Sci 7:4898–4917
13. Praveen BM, Venkatesha TV (2011) Electro-deposition and corrosion resistance properties of Zn-Ni/Tio_2 nano composite coating. Inter J Electrochem 261:407–410
14. Rahman et al (2009) Morphology and properties of electrodeposited Zn-Ni alloy coatings on mild steel. J Mech Eng Tran 40:9–15
15. Zheng HY, An MZ, Lu JF (2008) Surface characterization of the Zn-Ni-Al_2O_3 nanocomposite coating fabricated under ultrasound condition. Appl Surf Sci 34(254):1644–1650
16. Aziz M, Scheinder W, Plieth W (2005) Electrolytic co-deposition of silicate and mica particles with zinc. J Solid State Electrochem 9: 429–437
17. P. Wang, Y, Z Cheng, A Zhang (2011) Study on the electrocodeposition processes and properties of Ni-SiC nanocomposite coating. J. of Coat. Techn. Res. 8(3) 409–417
18. Tan C et al (2008) Nickel co-deposition with SiC particle at initial stage. Tran Nonferrous Met Soc China 18:1128–1133
19. Frade T et al (2010) Pulsed-reverse current electrodeposition of Zn and Zn-TiO_2 nanocomposite films. Surf Coat Technol 204:3592–3598
20. Zhang W, Liu W, Wang C (2002) Characterization and tribological investigation of sol–gel Al_2O_3 and doped Al_2O_3 films. J Euro Cer Soc 22:2869–2876
21. Abdel A, Barakat MA, Mohamed RM (2008) Electrophered Zn-TiO_2-ZnO nanocomposite coating films for photocatalytic degradation of 2-chlorophenol. Appl Surf 254:4577–4583
22. Fustes J, Gomes ADA, Silva Pereira MI (2008) Electrodeposition of Zn-TiO_2 nanocomposite films—effect of bath composition. J Solid State Electrochem 121(11):1435–1443
23. Dong D et al (2009) Preparation and properties of electroless Ni-P-SiO_2 composite coatings. Applied Surf Sci 255:7051–7055
24. Hu C, Wang C (2006) Effects of composition and reflowing on the corrosion behavior of Sn–Zn deposits in brine media. Electrochim Acta 51:4125–4134

25. Fayomi OSI et al (2013) Properties evaluation of ternary surfactant-induced Zn-Ni-Al_2O_3 films on mild steel by electrolytic chemical deposition. J Ovonic Res 9(5):123–132
26. Blejan D, Muresan LM (2012) Corrosion behavior of Zn-Ni-Al_2O_3 nanocomposite coatings obtained by electrodeposition from alkaline electrolytes. Mat Corro 63:1–6
27. Shivakumara S et al (2007) Influence of additives on electrodeposition of bright Zn–Ni alloy on mild steel from acid sulphates bath. Bulletin Mat Sci 30:455–462